Quantitative Determination of the Number of Secondary and Tertiary Structure Base Pairs in Transfer RNA in Solution†

P. H. Bolton, C. R. Jones, D. Bastedo-Lerner, K. L. Wong, and D. R. Kearns*

ABSTRACT: Resonances in the low-field (11–15 ppm) nuclear magnetic resonance spectrum (NMR) of tRNA molecules arise from secondary and tertiary structure base pairs (1 resonance for each base pair) as well as tertiary structure hydrogen bonds. An accurate method for integrating the low-field spectra has been developed and applied to seven different tRNA. In the presence of high levels of magnesium (10 mM free magnesium) the number of resonances (base pairs) per molecule is typically 3–4 more than the number predicted by the cloverleaf model. These results confirm our recent proposal that, under proper conditions, most tRNA exhibit 3–4 tertiary structure interactions in solution, which are also observed in x-ray diffraction studies of yeast $tRNA^{Phe}$. In addition to common resonances in the 11–15 ppm region, there are common resonances at 10.5 and 9.5 ppm. A critique of methods used to integrate the low-field spectra is given and possible sources of error are indicated. The discrepancy between our present results and previous studies, which indicated that the number of base pairs per molecule was close to the number predicted by the cloverleaf model, can be attributed partly to differences in magnesium concentration and partly to inaccuracies inherent in the integration methods used.

The first tRNA was sequenced about 10 years ago and at that time Holley proposed the now familiar cloverleaf structure (Holley et al., 1965). Since then, there has been interest in determining the secondary structure (i.e., the cloverleaf model) and the folding of the arms of the tRNA molecules (tertiary structure) in crystals and in solution (Gauss et al., 1971; Sigler, 1975). Of the various techniques that have been used, NMR[1] is especially well suited for investigating the base pairing structure of tRNA molecules in solution, since resonances in the low-field spectral region (11–15 ppm) can be used to directly monitor individual base pairs of the molecules (Kearns and Shulman, 1973). Each Watson–Crick base pair, and some tertiary structure base pairs, contribute one resonance (due to hydrogen-bonded ring nitrogen protons of G and U) to this spectral region, so, in principle, the total number of base pairs per molecule can be directly determined from integration of the low-field spectrum.

While seemingly simple, integration of the low-field spectra of tRNA has been difficult due to lack of an accurate intensity standard. Initially, we integrated spectra by comparison with an external standard (Kearns et al., 1971a,b) or with a resolved resonance(s) in the low-field region that was *assumed* to have a known intensity (Shulman et al., 1973b; Lightfoot et al., 1973). Neither method was completely satisfactory and the results indicated that several class I tRNA contained ~19 base pairs (not counting GU pairs), or about the number predicted by the cloverleaf model. We also found we were able to analyze the spectra of some seven different tRNA, assuming only the cloverleaf structure base pairs were present, and on this basis concluded that we had no (positive) evidence for the presence of additional tertiary structure base pairs, *under the conditions used in those experiments* (Kearns and Shulman, 1973; Shulman et al., 1973a,b; Lightfoot et al., 1973; Kearns et al., 1974).

However, other considerations indicated that resonances from tertiary structure base pairs might also be present under the appropriate experimental conditions. Levitt (1969) noted that tRNA contain a number of homologous bases in single-stranded regions of the tRNA cloverleaf model and, on the basis of these homologies and photochemical cross-linking data (Favre et al., 1971), proposed a number of tertiary structure base pairs that would be common to most class I tRNA. More importantly, the x-ray diffraction results on yeast $tRNA^{Phe}$ clearly indicate that many of the homologous bases are close enough to be hydrogen bonded (Kim et al., 1974b; Robertus et al., 1974). (At the present resolution, the x-ray data are not accurate enough to prove that they are actually hydrogen bonded.) Quite independent of the x-ray results, we discovered evidence in the NMR spectra of *Escherichia coli* tRNA for a resonance from a common tertiary structure base pair involving s^4U_8 and A_{14} (Wong and Kearns, 1974b). Reid et al. (1975) subsequently confirmed this assignment and presented evidence for additional resonances from tertiary interactions in *E. coli* $tRNA^{Val}$. Using mixed tRNA, we were able to identify common resonances in the lowfield spectra of mixed yeast and *E. coli* tRNA at 13.8, 13.0, and 11.5 ppm, which exhibit a sensitivity to magnesium and temperature expected for tertiary structure base pairs (Bolton and Kearns, 1975). The resonances located at 13.8 and 13.0 ppm are assigned to the T_{54}·A_{58} and G_{19}·C_{56} tertiary structure base pairs, respectively, and the one at 11.5 ppm is now assigned to a protected U in the anticodon loop (Kearns, 1976). Hilbers and Shulman (1974) in their study of *E. coli* $tRNA^{Glu}$ found evidence for an early melting resonance that they attributed to a G·C tertiary structure base pair, and, very recently, Robillard et al. (1976) discussed NMR evidence for tertiary interactions in yeast $tRNA^{Asp}$.

The assignment of resonances from tertiary structure base pairs implies that most tRNA should contain on the order of 3–4 more resonances in the low-field region than the number predicted by the cloverleaf model. This contradicts earlier results that indicated that the number of base pairs is approximately equal to that required by the cloverleaf model (Kearns et al., 1971a,b; Shulman et al., 1973a,b; Lightfoot et al., 1973). Because of limitations in our earlier integration

† From the Department of Chemistry, Revelle College, University of California, San Diego, La Jolla, California 92093. *Received December 16, 1975.* This work was supported by a grant from the United States Public Health Service (GM 21431).

[1] Abbreviations used are: NMR, nuclear magnetic resonance; EDTA, (ethylenedinitrilo)tetraacetic acid.

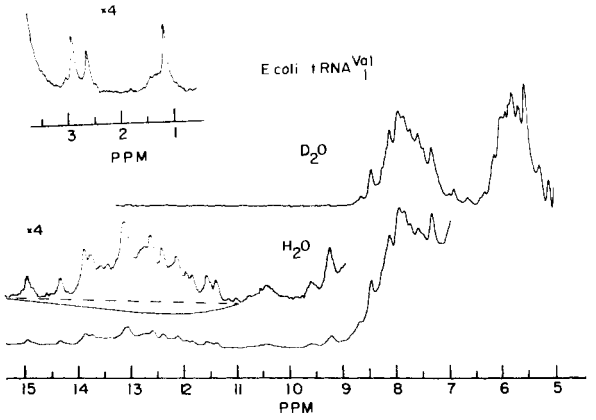

FIGURE 1: 300 MHz spectrum of tRNA^{Val} under various experimental conditions. The spectrum at the bottom of the figure is that of tRNA^{Val} under normal NMR conditions, that is, dialyzed against 0.1 *M* NaCl, 10 mM $MgCl_2$, and 10 mM $K_2H_2PO_4$, pH 7.0. The spectrum of the methyl region (upper left) was also obtained under these conditions. The sample was then dried to 0.33–0.25 of its original volume and brought to its original volume with D_2O. This procedure was repeated several times until the sample was 95–98% D_2O. The spectrum of the aromatic region was obtained with the D_2O sample under identical experimental conditions as the H_2O sample. The methyl region of the spectrum was also investigated for the D_2O sample and the intensity was compared to that of the H_2O sample. The intensities agreed to within 5%, indicating there was no loss of the sample during the solvent change. The aromatic region contains 89 protons. Using the dashed baseline the low-field region contains 23 protons, whereas use of the solid baseline gives an intensity of 26 protons for the low-field region. The dashed baseline is the more reasonable (see text).

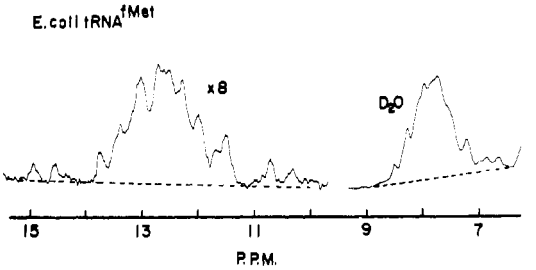

FIGURE 2: 300 MHz NMR spectrum of *E. coli* tRNA$^{Met}_f$ under various experimental conditions as described in Figure 1.

methods, part of the discrepancy could be due to errors inherent in the integration methods themselves. Alternatively, it was possible that the low numbers of base pairs we originally obtained were due to the fact the measurements were carried out under conditions ($T \simeq$ 35–45 °C, 3–5 mM Mg) where some resonances from tertiary interactions begin to melt out (Bolton and Kearns, 1975). In view of these problems and the important role that integration plays in any detailed interpretation of the low-field NMR spectra of tRNA, we have developed a new, more accurate, method for integrating the low-field spectra. A more accurate integration method was also desirable in order to correlate the NMR results with the results of the x-ray diffraction studies on yeast tRNA^{Phe} and to determine the extent to which all, or most, tRNA have the same tertiary structure in solution. A preliminary account of our observations obtained using a new integration method on *E. coli* tRNA$^{Val}_1$ was presented earlier (Kearns et al., 1975). In the present paper, we present the results on seven different tRNA. These new results confirm that, in the presence of sufficient levels of magnesium, most tRNA contain about 3–4 additional resonances between 11.5–15 ppm from tertiary structure interactions. In addition to the common resonances previously reported, we find two more resonances in the 11.5–9.5 ppm region which are common to most tRNA. A critique of the integration methods is also given and the effect of magnesium on the integration is reported.

Experimental Section

(a) *tRNA Samples. E. coli* tRNA$^{Met}_f$ and tRNA$^{Val}_1$ were purified to a specific activity of at least 1.4 nM/A_{260} unit by chromatography on BD-cellulose (Gilliam et al., 1967) and RPC-7 (Isham and Stulberg, 1974). *E. coli* tRNA$^{Tyr}_{1,2}$ and tRNA^{Asp} and yeast tRNA^{Phe} were purified on BD-cellulose (Gilliam et al., 1967) and RPC-5 (Pearson et al., 1970) to specific activities of at least 1.4 and 1.5 nM/A_{260} unit, respectively. *E. coli* tRNA$^{Glu}_2$ was the gift of A. D. Kelmers, Oak Ridge National Laboratories, and *E. coli* tRNA$^{Trp}_{su+}$ was supplied by R. H. Buckingham and the analysis of its spectrum will be discussed elsewhere. Amino acid acceptance assays were performed under standard conditions. The *E. coli* tRNA used in this investigation were less than 5% photocross-linked as determined by the absorption of the $NaBH_4$ reduced RNA at 377 nm (Ofengand and Bierbaum, 1973).

After purification, tRNA samples were precipitated with ethanol and stored at −20 °C. NMR samples were prepared by dissolving the precipitate in 0.1 M NaCl and 10 mM EDTA and heating the sample to 75 °C followed by a slow cooling (2–3 h) to room temperature. The samples were then vacuum dialyzed against 0.1 M NaCl, 10 mM $MgCl_2$, and 10 mM $K_2H_2PO_4$ or 10 mM cacodylate at pH 7.0. Samples prepared in the absence of magnesium were dialyzed against the above buffer with the magnesium left out, but with the addition of 2 mM EDTA. The final concentration of the tRNA samples was 1–2 mM.

(b) *NMR Spectra.* NMR spectra were obtained with a Varian HR-300 spectrometer operated in the field sweep mode. Spectra were scanned at 2000 Hz/15 s and signal averaged with a Nicolet 1020A for 2–3 h. Baselines were corrected, where shown, by a computer program prepared by Mr. T. Early of our group.

(c) *Integration Procedure.* Although we have used four other methods for integrating the low-field region of the spectra (Kearns and Shulman, 1973; Kearns et al., 1971a,b; Lightfoot et al., 1973), we believe more accurate results are obtained by comparing the intensity of the appropriate low-field region with that of the aromatic region, 6.5–8.5 ppm. The number of resonances in the aromatic region is easily predicted from the sequence, since there are two resonances for each adenine and just one for each of the other common bases. While the positions of the resonances from some of the rare bases may be uncertain, this will lead to an error of at most a few percent. The spectral region included in the integration must be carefully chosen, since resonances from several aromatic protons almost overlap with resonances from ribose protons. On the basis of studies of various natural and synthetic polynucleotides and computations (Early, unpublished results), we compute that the most upfield shifted aromatic resonances will occur at ~6.5 ppm. Consequdeuy, integration of the spectra from 8.5 to 6.5 ppm will include all of the expected aromatic protons.

In order to observe resonances from exchangeable ring nitrogen protons in the low-field region, the experiments must be performed in H_2O. However, to determine the intensity in the aromatic region of the spectra the measurements must be performed in D_2O to eliminate resonances from the exchangeable amino protons which also occur in the aromatic region. In the actual experiments, the spectra are first measured in H_2O in both the lowfield and aromatic regions. The

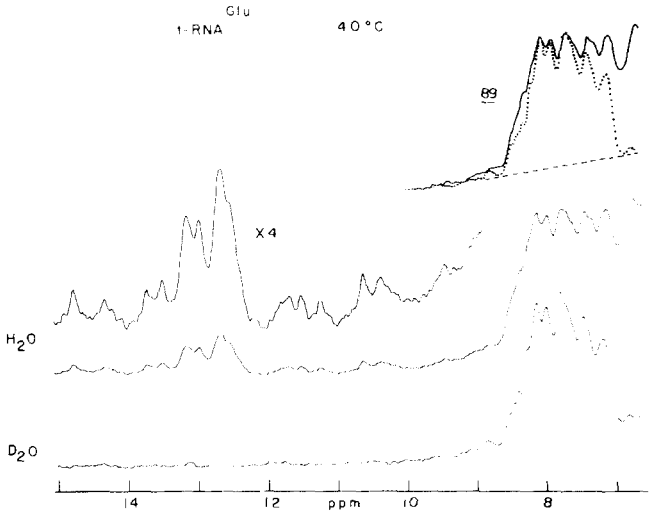

FIGURE 3: 300 MHz NMR spectrum of *E. coli* $tRNA^{Glu}_{1,2}$ under various experimental conditions as described in Figure 1. The D_2O and H_2O spectra in the aromatic region are shown superimposed in the upper right of the figure.

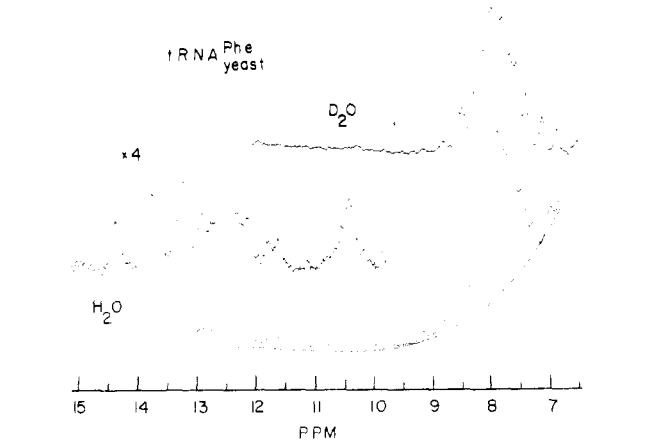

FIGURE 4: 300 MHz NMR spectrum of yeast $tRNA^{Phe}$ under various experimental conditions as described in Figure 1.

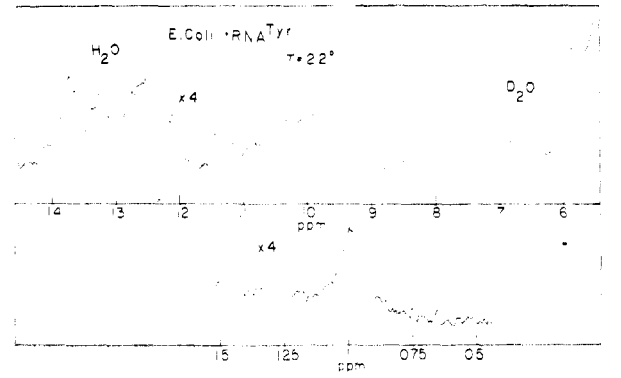

FIGURE 5: 300 MHz NMR spectrum of *E. coli* $tRNA^{Tyr}$ under various experimental conditions as described in Figure 1.

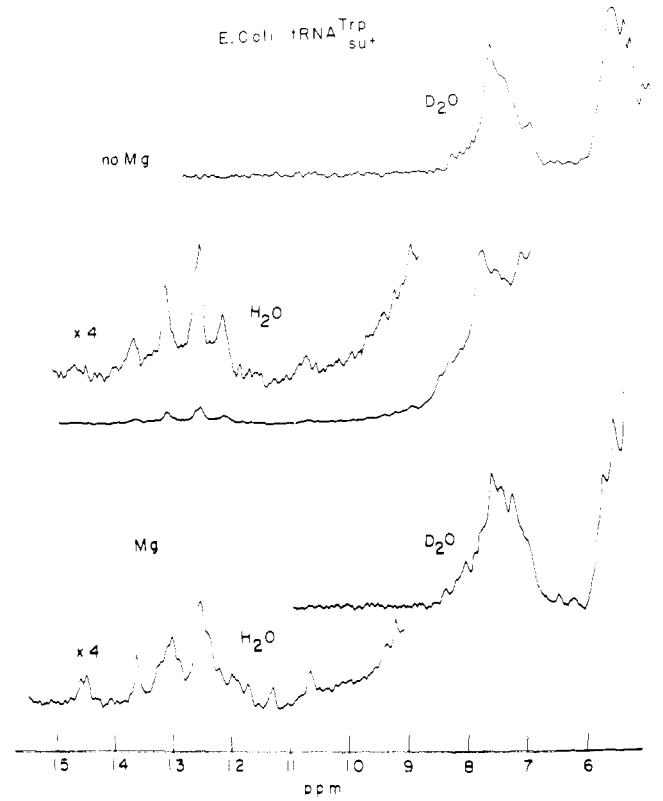

FIGURE 6: 300 MHz NMR spectrum of *E. coli* $tRNA^{Trp}_{su+}$ under various experimental conditions as described in Figure 1. The spectrum in the absence of magnesium (no Mg) was obtained in the same manner as the magnesium-containing samples except that the magnesium was removed by the addition of excess EDTA, ~10 mM EDTA/Mg.

sample is then reduced to 0.33–0.25 its original volume by a stream of dry, filtered, nitrogen and returned to its original volume with D_2O. This process is repeated several times until the sample is 95–98% D_2O. The spectrum in the aromatic region is then remeasured using identical instrument settings as were initially used to obtain the spectrum in H_2O. The two spectra are then compared and the intensity in the low-field region is computed on the basis of the number of resonances predicted for the aromatic region. The results of these measurements on six tRNA are shown in Figures 1–6 and in Table I. In order to demonstrate that the conversion from H_2O to D_2O does not affect the tRNA concentration, spectra in the methyl region (1–3 ppm) (Kan et al., 1974; Kastrup and Schmidt, 1975; Kearns et al., 1975; Daniel and Cohn, 1975; Reid and Robillard, 1975) were obtained before and after solvent conversion. Since there are no exchangeable resonances from tRNA in the methyl region, the intensity of the methyl resonances should be the same in D_2O as in H_2O and our experiments show that this is indeed the case to better than 5%.

As an internal check on the accuracy of this method, we also compared the intensity in the aromatic region with that located between 6.4 and 5.0 ppm (Figure 7). Resonances in this latter region are due to the Cl′ ribose protons, one per residue, and one from each of the H_5 protons of C and U (ring current calculations show that 3–6 of the C or U resonances may be shifted to still higher field). The results of such a comparison (Table II) show that there is excellent agreement between the experimental and calculated values. This test also eliminated the unlikely possibility that resonances from some of the ribose protons have been anomalously downfield shifted into the aromatic region or vice versa. For example, if just five of the ribose or H_5 resonances of C or U were shifted into the aromatic region the calculated ratio, aromatic/ribose, would typically be increased from 90/90 to 95/85. This would produce an error of 12%, which is much larger than the error involved in comparing these two regions of the spectra.

TABLE I: Summary of the Results of Integrations of the Low-Field NMR Spectra of tRNA.

tRNA Species (No. of Cloverleaf Watson-Crick Base Pairs)	Magnesium Concn.	t (°C)	Integration Method	No. of Low-Field Resonances
Yeast $tRNA^{Phe}$	~2 mM	24	External[e]	21 ± 3
(20)	10 mM dialyzed	36	Internal[f]	1
9.6				
	10 mM total	37	Internal[g]	18.5
	10 mM dialyzed	40	Aromatic[a]	22.2 ± 1
E. coli $tRNA^{Met}_f$	3 mM	40	External[i]	23 ± 2
(19)	5 mM	24	Internal[h]	19
	5 mM dialyzed	37	Internal[d]	27
	10 mM dialyzed	37	Aromatic[a]	23 ± 1
E. coli $tRNA^{Glu}_{1,2}$	10 mM	40	Internal[h]	20
(20,19)	10 mM dialyzed	40	Aromatic[a]	21.5 ± 1
E. coli $tRNA^{Val}_1$	15 mM	37	Internal[b]	26 ± 3
(19)	10 mM dialyzed	35	Aromatic[a]	23 ± 1
	15 mM	37	Internal[c] methyl	26 ± 1
Yeast $tRNA^{Asp}$	15 mM	37	Internal[j]	20
(17)				
E. coli $tRNA^{Asp}$	10 mM dialyzed	40	Aromatic[a]	20.2 ± 1
(18)				
E. coli $tRNA^{Trp}_{su+}$	40 mM	40	Aromatic[a]	22 ± 1
(20)	3 mM	40	Aromatic[a]	19 ± 1
E. coli $tRNA^{Tyr}_{1,2}$	10 mM dialyzed	37	Aromatic[a]	26 ± 2
(23)				

[a] This paper. [b] Reid et al., 1975. [c] Reid and Robillard, 1975. [d] Daniel and Cohn, 1975. [e] Kearns et al., 1971a. [f] Jones, C. R., unpublished results. [g] Lightfoot et al., 1973. [h] Shulman et al., 1973b. [i] Kearns et al., 1971b. [j] Robillard et al., 1976.

TABLE II: Comparison of the Calculated and Observed Ratio of the Intensities in the Aromatic (9–6.5 ppm) and Ribose (6.5–5.0 ppm) Regions of the Spectra of tRNA.

tRNA Species	Relative Intensity (ribose/aromatic) Calcd	Obsd
E. coli $tRNA^{Glu}$	1.25	1.20
E. coli $tRNA^{Met}_f$	1.27	1.27
E. coli $tRNA^{mixed}$	1.27	1.32

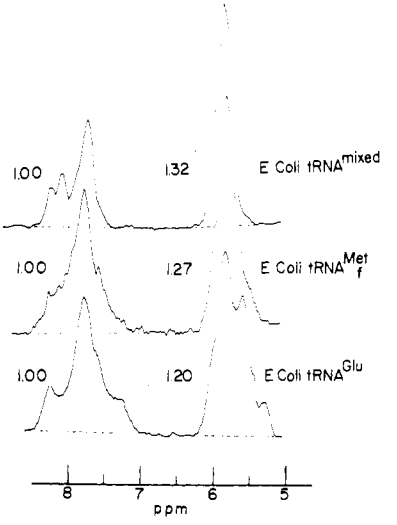

FIGURE 7: 300 MHz NMR spectra of *E. coli* $tRNA^{Glu}_{1,2}$, $tRNA^{Met}_f$, and unfractionated *E. coli* tRNA in the 9–5 ppm region.

Results and Discussion

Before examining the integration results and discussing their implications with regard to the tertiary structure of tRNA molecules in solution, we present a critique of integration methods used previously and consider some potential errors in the new method.

Critique of Integration Methods. (a) External Standards. In our initial tRNA studies, metcyanomyoglobin was used as a reference for integration of the low-field region of tRNA spectra (Kearns et al., 1971a,b). One problem with this method is that two different samples of known concentration must be prepared and their spectra accurately compared. There are additional problems in using a standard with a single resolved resonance (see discussion below).

(b) Internal (Added) Standards. We have attempted to use various compounds (e.g., phenanthroline complexes of Co^{2+}) that are added to tRNA samples and that exhibit a resonance well resolved from those of the tRNA. While this method eliminates problems arising from drift in spectrometer intensity, the difficulty of accurately determining the concentration of *both* the standard and the tRNA remains. Furthermore, most of the compounds we have examined were inorganic salts and there were invariably problems due to interaction with the tRNA.

(c) Resolved Low-Field Resonances of tRNA as Internal Standards. A third method we (Shulman et al., 1973b; Lightfoot et al., 1973) and others (Daniel and Cohn, 1975; Reid and Robillard, 1975) have used to integrate tRNA spectra is to *assume* that one or more resonance in the low-field region of the spectrum corresponds to an integral number of protons. When carefully used, this method may give reasonable values, though there are a number of potential problems. First, resonances from tertiary structure base pairs are located throughout the low-field region of the spectrum and these are very sensitive to temperature, as well as to the magnesium concentration. Thus, depending upon experimental conditions,

tertiary structure base pairs could be partially melted out and this would lead to nonintegral intensity in some peaks. Second, many *E. coli* tRNA are easily photo-cross-linked and/or photooxidized and this can lead to errors in integration, particularly if the resonance from the s^4U_8·A_{14} tertiary structure base pair is used as an internal standard (Wong and Kearns, 1974b; Wong et al., 1975). There is the additional problem that, when the resonances have a Lorentzian line shape, it is extremely difficult to draw a proper baseline for a single, partially resolved, resonance that is located near a large collection of resonances. (To the extent permitted by the signal to noise the line shapes of a number of tRNA species are well accounted for by Lorentzian lines (Jones et al., 1976, Rordorf et al., 1976).) According to theory, it is necessary to integrate over $6\Delta\nu_{1/2}$ to include 90% of the true intensity of a Lorentzian resonance with a half-width of $\Delta\nu_{1/2}$. In order to include 95% of the intensity, the integration must be over $12\Delta\nu_{1/2}$. Unless the resonances are well separated from each other, and the signal to noise ratio is extremely good, this is not possible. In the tRNA spectra, it is not feasible to include more than about 150 Hz in the integration of even the most well resolved resonances because of overlap from neighboring resonances, as well as the signal to noise ratio limitations. Hence, the area assigned to any individual resonance could be at least 10% smaller than its true intensity. Conversely, when the area in the entire low-field spectrum is measured, the integration is over 900 Hz and all peaks (except resonances at the extremes of the spectra) are given full weight. In this way, use of partially resolved resonances (necessarily integrated over a limited range), as a standard to integrate the entire low-field spectrum covering over 900 Hz, can give an incorrect value. The same considerations also apply to the use of resonances from methyl protons to integrate spectra.

(d) Methyl Proton Resonances as Internal Standards. Resonances from methyl protons have recently been used as an internal intensity standard by another group (Reid and Robillard, 1975) who obtained values for the intensity in the low-field region of $tRNA^{Val}_1$ which are somewhat higher than the values which we obtained (Kearns et al., 1975). One problem with using methyl resonances to integrate spectra can be understood in terms of the high-field spectrum of $tRNA^{Val}_1$, which is shown in Figure 1 along with the spectra obtained in the low-field, aromatic, and ribose regions. The resonances at 1.07, 2.55, and 2.85 ppm have full width at half-height of 35 Hz, which is comparable to the width observed in the low-field region. To integrate the resonances, a choice must be made regarding the spectral width to be included and the probable baseline. As shown in Figure 1, the sharp peak at 1.07 ppm, assigned to the methyl group of rT_{54}, appears to be superimposed on a broader peak. If the area contained just within the sharp peak (approximately an 80-Hz region) is assumed to correspond to three protons, the integration indicates there are 29 protons in the low-field region between 11.5 and 15 ppm. On the other hand, if the entire intensity located between 0.9 and 1.5 ppm is used, we find only 20 low-field protons. Clearly, the exact and somewhat arbitrary choice of the baseline and spectral range used in the integration of the methyl peak has a pronounced effect on the intensity determined for the low-field region of the spectrum. The peaks at 2.85 and 2.55 ppm have intensities in the approximate ratio of 3:2 and the spectrum in Figure 1 shows that a broad background underlies these peaks.

Another problem in using the methyl resonances is that this region of the spectrum is particularly susceptible to non-tRNA impurities (Kastrup and Schmidt, 1975). The tRNA concentration is typically on the order of 1–2 mM so that a small amount of contamination can have a pronounced effect on this region of the spectrum. In their investigation of the methyl resonances of *E. coli* $tRNA^{Val}_1$, Kastrup and Schmidt (1975) found several impurities that had been introduced during the isolation of the tRNA that gave rise to resonances in this region. Impurities that are apparently responsible for some of the extra peaks in the high-field spectrum of *E. coli* $tRNA^{Val}_1$ reported by Reid and Robillard (1975) and by Kastrup and Schmidt (1975) are absent in our spectrum shown in Figure 1.

Incomplete methylation and modification of bases is yet another source of error, since it is known that the degree of methylation of the rare bases in tRNA ranges from 65–115% and varies from residue to residue in the same tRNA (Singhal and Best, 1973). Extra hU residues are present in some tRNA and these give rise to resonances in the methyl region (Chambers, unpublished results).

Finally, there is the technical problem of signal to noise ratio. While this may be partially overcome by extensive signal averaging, the use of a region with more intensity naturally leads to a better signal to noise ratio and hence a more accurate determination of the intensity of the region.

The "tailing" of the Lorentzian lines and incomplete methylation combine to diminish the integrated intensity of the methyl protons, whereas contributions from impurities have the reverse effect. Thus, when methyl resonances are used as an intensity standard to integrate the low-field region, an error of ±10–20% is possible unless precautions are taken to remove impurities and the extent of methylation of the sample is carefully determined. Even then the problem of the integration of a Lorentzian line remains.

(e) Aromatic Protons as Internal Standards. In the present paper, we have used resonances in the aromatic region (8.5–6.5 ppm) to integrate spectra. This method offers a number of advantages over the methods discussed above. The number of resonances in the aromatic region is known from the primary sequence. The intensity of the aromatic region typically corresponds to 85–100 protons/molecule, so the signal to noise ratio is high and the presence of contaminating material is much less serious. Similarly, the presence (or absence) of rare bases will have only a small effect on the total intensity of the aromatic region. A very important advantage in using the aromatic region to calibrate the low-field region lies in the fact the two regions are integrated over similar spectral ranges (2 vs. 3.5 ppm) and both regions contain numerous overlapping resonances. In this way, the problems encountered using resolved low-field or methyl resonances are eliminated, since the integration is over 15 or 20 times the line width of an individual resonance.

Considering again the $tRNA^{Val}_1$ spectrum shown in Figure 1, it is clear that there is no ambiguity as to where the baseline should be drawn to integrate the aromatic region of the spectrum. Likewise, the choice of baseline for the low-field region is fairly obvious. A second, obviously poorer, baseline for the low-field region is also shown to demonstrate the sensitivity of the integration to choice of baseline.

The method is not without possible sources of error and these need to be considered.

(i) Ribose or Aromatic Protons with Anomalous Shifts. Special folding of the tRNA molecules could induce anomalous downfield shifting of some ribose protons from their expected position at 6.4–5 ppm into the aromatic region. Conversely, some resonances from aromatic protons could be upfield shifted into the ribose region. To check these possibilities, we

measured the relative intensities in the aromatic and ribose regions of several tRNA and these results are shown in Table II and Figure 7. The ribose region contains one resonance from each C and U, as well as one from each ribose group in the molecule. The intensities in these two regions should therefore compare in an easily computed manner and the results shown in Table II demonstrate that the agreement between experimental and computed values is excellent.

(ii) Impurity Contamination. The aromatic region could also be contaminated by impurities, but the results presented above place strict limitations on the nature of the impurity. Since the ratio of intensities of the aromatic and ribose region of the impurity must be very similar to that calculated for the tRNA, the only impurities that could reasonably satisfy this requirement are mono- or oligonucleotides. The presence of such contaminants can be ruled out for the following reasons. The acylation of the tRNA indicates that at least 90–95% of the uv-absorbing material is tRNA. In addition, several of the tRNA samples used in the integrations were also examined on polyacrylamide gels under denaturing conditions and no evidence was found for contamination of the tRNA by material that absorbed at 260 nm. The gel experiments also rule out the possibility that the samples are contaminated by high-molecular-weight impurities. Thus, it appears unlikely that the tRNA samples used in the integrations have more than 1–2 contaminating aromatic resonances per tRNA. Since the intensity of the aromatic region is about four times larger than that of the low-field region, it would take intensity corresponding to 4 resonances/tRNA to give an error of 1 base pair/molecule in the integration of the low-field region. The comparison of the intensity of the aromatic and ribose regions and the fact that we find no evidence for aromatic contaminants in our samples indicate that impurities cause an error of at most ~0.5 of a resonance in our determination of the intensity of the low-field region.

(iii) Differential Saturation of Aromatic Protons or Low-Field Protons. We have collected low-field spectra using a wide range of rf power and find that the power levels used in the present experiments are well below that required to saturate any resonances in the low-field or aromatic region. Saturation of the aromatic resonances would lead to an intensity in the low-field that is too high.

(iv) Resonances from Amino Protons in the Aromatic Region. Model compound studies and comparison of spectra obtained in H_2O and D_2O indicate that resonances from amino protons are located between 6–9 ppm. Although these exchangeable protons are not observed in D_2O, the residual water content (~5%) could result in some intensity in the aromatic region due to the amino protons. This contribution would be quite small, since experiments have shown that the ratio of aromatic to amino protons is about 4:1, so in 95% D_2O the contribution of the amino protons will be negligible.

We conclude that the use of the aromatic protons to calibrate the intensity of the low-field region avoids many of the difficulties associated with methods previously used and should lead to highly accurate values for the number of resonances in the low-field region of the spectrum. We have applied this method to a number of different tRNA and the results are shown in Table I. The following considerations indicate the error in these values is less than ±2 base pairs/molecule and probably closer to ±1 base pair/molecule. When repeated measurements are made on separate samples, several days apart and at different tRNA concentrations, the values for the integration agree to within ±0.5 base pair/molecule (e.g., *E. coli* $tRNA^{Val}_1$ 22.7–23.3). Measurements carried out by different persons on the same tRNA using different sample preparations gave values that agreed to within 0.5 base pair/molecule. While reasonable baselines can give values that differ by about 1 base pair/molecule, in order to obtain values which differ by ±2 base pairs, unreasonable baselines have to be chosen (e.g., see Figure 1).

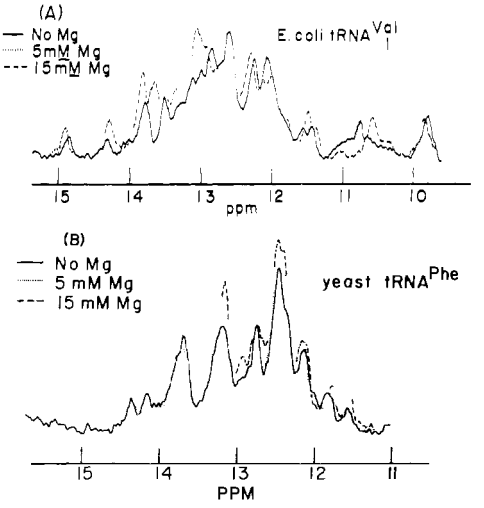

FIGURE 8: 300 MHz NMR spectra of yeast $tRNA^{Phe}$ (A) and *E. coli* $tRNA^{Val}_1$ (B) in the presence of various amounts of magnesium at 35 °C. The samples were prepared by dissolving desalted tRNA in 0.1 M NaCl, 10 mM $K_2H_2PO_4$, pH 7.0. The intensity of the $tRNA^{Val}_1$ spectrum corresponds to 20 ± 1 (no Mg), 21.5 ± 1 (5 mM Mg), and 23 ± 1 (15 mM Mg). The intensity of the $tRNA^{Phe}$ spectrum corresponds to 19.8 ± 1 (no Mg), 21.1 ± 1 (5 mM Mg), and 22.2 ± 1 (15 mM Mg) protons per molecule.

Integration Results: 11–15 ppm Region. When aromatic protons are used to integrate the low-field spectra of tRNA, which have been dialyzed against 10 mM magnesium, the number of resonances in the low-field region is found to vary from 21 (*E. coli* $tRNA^{Glu}_2$) to 26 (*E. coli* $tRNA^{Tyr}$). With a couple of exceptions, there are 3–4 more resonances than predicted by the cloverleaf model and this agrees with our results that indicate 3–4 resonances from common tertiary structure interactions. Our value for *E. coli* $tRNA^{Val}_1$ (23 ± 1) is slightly less than the value of 26 ± 1 recently reported by Reid and Robillard (1975) and we have discussed the possible basis for the discrepancy above. Daniel and Cohn (1975) recently obtained a value of 27 (compared with our value of 23 ± 1) for *E. coli* $tRNA^{Met}_f$ by making assumptions about certain resolved resonances observed in the low-field spectra, and we have discussed the problems with this method. Aside from these relatively small differences, it would appear that there is convincing NMR evidence that, under the proper experimental conditions, the majority of tRNA do contain extra base pairs in addition to those from the cloverleaf secondary structure.

One final point that needs to be clarified is why earlier NMR integrations lead to somewhat lower values (19–20 compared with 22–23) for the total number of base pairs (Kearns and Shulman, 1973; Shulman et al., 1973b; Lightfoot et al., 1973). To determine the extent to which the errors in the previous integrations are due to magnesium deficiency and/or problems with the previous techniques, we have examined two pure tRNA under conditions that closely approximate the experimental conditions used previously. As the spectra in Figure 8 show, there is a gain of intensity upon the addition of 5 mM Mg to a sample containing no magnesium and the further addition to 15 mM Mg induces the gain of about 1–2 additional resonances in the low-field region. The experiments that gave 19

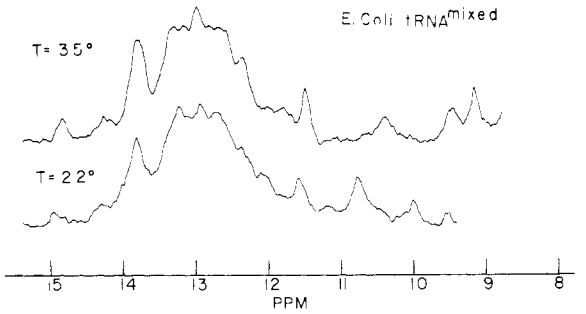

FIGURE 9: 300 MHz NMR spectrum of *E. coli* $tRNA^{mixed}$ at 22 and 35 °C. The tRNA was prepared by dialysis against 10 mM $MgCl_2$, 10 mM $K_2H_2PO_4$, and 0.1 M NaCl. The common resonances at 14.9, 13.8, 13.0, and 11.5 ppm have been discussed elsewhere (Bolton and Kearns, 1975). The spectra shown clearly demonstrate that there are additional common resonances in the 11–9 ppm region. The resonance that is originally at 10.8 ppm at 22 °C broadens and shifts to 10.5 ppm at 35 °C. The resonances at 9.4 and 9.1 ppm are not observable in the 22 °C spectrum due to the tailing of the water peak. The assignments of these resonances are discussed in the text.

TABLE III: Summary of the Assignments of Resonances from Common Tertiary Structure Base Pairs in Class I tRNA.

Obsd Resonance Position (ppm)	Tertiary Structure Base Pair[a]
14.8[b]	s^4U_8·A_{14}
14.3[c]	U_8·A_{14}
13.8	T_{54}·A_{58}
13.0	G_{19}·C_{56}
11.5	U_{33}
10.5	G_{15}·C_{48}(?)
9.5	?

[a] Numbering system for yeast $tRNA^{Phe}$. [b] *E. coli* tRNA. [c] Yeast tRNA.

resonances/molecule were performed under conditions of about 3–5 mM Mg. Since the spectra shown (Figure 9) demonstrate that addition of magnesium to tRNA under these conditions induces the gain of intensity corresponding to about 2 protons/molecule, it appears that about one-half of the error in the previous results (2 resonances/molecule) is due to the lack of magnesium. The rest of the error must be attributed to the less accurate integration methods used.

Relation between the Structure of tRNA in Solution and the Structure of Yeast $tRNA^{Phe}$ in the Crystal. Two very important questions have been generated by the determination of the crystal structure of yeast $tRNA^{Phe}$. To what extent is the structure of $tRNA^{Phe}$ the same in the crystal as in solution? What is the relation between the solution structure of $tRNA^{Phe}$ and other class I tRNA? Recent NMR studies of various pure tRNA and mixtures of tRNA have found 3–4 extra resonances in the low-field spectrum which are common to most tRNA (Wong and Kearns, 1974a,b; Wong et al., 1975; Bolton and Kearns, 1975). The results reported here confirm that under the proper experimental conditions (adequate levels of magnesium) the class I tRNA do contain more base pairs than would be expected simply on the basis of the cloverleaf model. In most cases, it is possible to make plausible assignments of the extra resonances in terms of tertiary structure base pairs deduced from x-ray diffraction studies of yeast $tRNA^{Phe}$. The common resonances of *E. coli* tRNA at 14.9, 13.8, 13.0, and 11.5 ppm have been assigned to s^4U_8–A_{14}, A_{58}–T_{54}, G_{19}–C_{56}, and U_{33}, respectively. The U_{33} is thought to have its ring nitrogen proton hydrogen bonded to phosphate 36 as is found in the crystal. In addition to these common resonances, we find evidence for other common resonances in the 11–9 ppm region as shown in Figure 9. Some resonances in this region have previously been attributed to GU pairs (Reid and Robillard, 1975), but this remains to be confirmed. Alternatively, these resonances could be assigned to common non-Watson–Crick tertiary structure base pairs that have ring nitrogen protons hydrogen bonded to carbonyl groups or to amino protons hydrogen bonded to ring nitrogens of the bases. Further work will be required to establish the assignments.

Taking all of the data together, we conclude that there is strong evidence that the majority of the class I tRNA have the same secondary and tertiary structure in solution and that this structure is the same as the one deduced for yeast $tRNA^{Phe}$ crystals. A summary of the assignments of resonances from the common tertiary structure base pairs is given in Table III.

References

Bolton, P. H., and Kearns, D. R. (1975), *Nature (London) 225,* 347–349.

Chambers, R. W. (unpublished results).

Chen, M. C., Giegé, R., Lord, R. C., and Rich, A. (1975), *Biochemistry 14,* 4385–4391.

Daniel, W. E., and Cohn, M. (1975), *Proc. Natl. Acad. Sci. U.S.A. 72,* 2582–2586.

Favre, A., Michelson, A. M., and Yaniv, M. (1971), *J. Mol. Biol. 58,* 367–379.

Gauss, D. H., von der Haar, F., Maelicke, A., and Cramer, F. (1971), *Annu. Rev. Biochem. 40,* 1045–1078.

Gilliam, I., Millward, S., Blew, D., von Tigestrom, M., Wimmer, E., and Tener, G. M. (1967), *Biochemistry 6,* 3043–3056.

Hilbers, C. W., and Shulman, R. G. (1974), *Proc. Natl. Acad. Sci. U.S.A. 71,* 3239–3242.

Holley, R. W., Apgar, J., Everett, G. A., Madison, J. T., Marquisee, M., Merrill, S. H., Penswick, J. R., and Aamir, A. (1965), *Science 147,* 1462–1465.

Isham, K. R., and Stulberg, M. P. (1974), *Biochim. Biophys. Acta 340,* 177–182.

Jones, C. R., Kearns, D. R., and Muench, K. H. (1976), *J. Mol. Biol. 103,* 747–764.

Kan, L. S., Ts'o, P. O. P., Haar, F. V. D., Sprinzl, M., and Cramer, F. (1974), *Biochem. Biophys. Res. Commun. 59,* 22–29.

Kastrup, R. V., and Schmidt, P. A. (1975), *Biochemistry 14,* 3612–3617.

Kearns, D. R. (1976), *Prog. Nucleic Acid Res. Mol. Biol. 18,* 91–149.

Kearns, D. R., Jones, C. R., Wong, K. L., Bolton, P. H., and Wolfson, M. (1975), "Conformation of tRNA in Solution", presented at EMBO Workshop on tRNA Structure and Function, Nof Ginossar, Israel, Feb. 24–29 (1975).

Kearns, D. R., Patel, D. J., and Shulman, R. G. (1971a), *Nature (London) 229,* 338–339.

Kearns, D. R., Patel, D., Shulman, R. G., and Yamane, T. (1971b), *J. Mol. Biol. 61,* 265–270.

Kearns, D. R., and Shulman, R. G. (1973), *Acc. Chem. Res. 7,* 33–39.

Kearns, D. R., Wong, Y. P., Cheng, S. H., and Hawkins, E. (1974), *Biochemistry 13,* 4736–4746.

Kim, S. H., Suddath, F. L., Quigley, G. J., McPherson, A., Sussman, J. L., Wang, A. H. J., Seeman, N. C., and Rich, A. (1974a), *Science 185,* 435–440.

Kim, S. H., Sussman, J. L., Suddath, F. L., Quigley, G. J., McPherson, A., Wang, A. H. J., Seeman, N. C., and Rich, A. (1974b), *Proc. Natl. Acad. Sci. U.S.A. 71,* 4970-4974.

Klug, A., Ladner, J. E., Robertus, J. D. (1974), *J. Mol. Biol. 89,* 511-516.

Ladner, J. E., Jack, A., Robertus, J. D., Brown, R. S., Rhodes, D., Clark, B. F. C., and Klug, A. (1975), *Nuc. Acids Res. 2,* 1629-1637.

Langlois, R., Kim, S. H., and Cantor, C. R. (1975), *Biochemistry 14,* 2554-2558.

Levitt, M. (1969), *Nature 224,* 759-763.

Lightfoot, D. R., Wong, K. L., Kearns, D. R., Reid, B. R., and Shulman, R. G. (1973), *J. Mol. Biol. 78,* 71-89.

Ofengand, J., and Bierbaum, J. (1973), *Biochemistry 12,* 1977-1984.

Pearson, R. L., Weiss, J. F., and Kelmers, A. D. (1970), *Biochim. Biophys. Acta 228,* 770-774.

Quigley, G. J., Seeman, N. C., Wang, H. J., Suddath, F. L., and Rich, A. (1976), (in press).

Reid, B. R., Ribeiro, N. S., Gould, G., Robillard, G., Hilbers, C. W., and Shulman, R. B. (1975), *Proc. Natl. Acad. Sci. U.S.A. 72,* 2049-2053.

Reid, B. R., and Robillard, G. T. (1975), *Nature (London) 257,* 287-291.

Robertus, J. D., Ladner, J. E., Finch, J. T., Rhodes, D., Brown, R. S., Clark, B. F. C., and Klug, A. (1974), *Nature (London) 250,* 546-551.

Robillard, G. T., Hilbers, C. W., Reid, B. R., Gangloff, J., Dirheimer, G., Shulman, R. G. (1976), *Biochemistry 15,* 1883-1888.

Rordorf, B. F., Kearns, D. R., Hawkins, E., and Chang, S. H. (1976), *Biopolymers 15,* 325-336.

Shulman, R. G., Hilbers, C. W., Kearns, D. R., Reid, B. R., and Wong, Y. P. (1973a), *J. Mol. Biol. 78,* 57-69.

Shulman, R. G., Hilbers, C. W., Wong, Y. P., Wong, K. L., Lightfoot, D. D., Reid, B. R., and Kearns, D. R., (1973b), *Proc. Natl. Acad. Sci. U.S.A. 70,* 2042-2045.

Sigler, P. B. (1975), *Annu. Rev. Biophys. Bioeng. 4,* 477-527.

Singhal, R. P., and Best, A. N. (1973), *Biochim. Biophys. Acta 331,* 357-368.

Wong, K. L., Bolton, P. H., and Kearns, D. R. (1975), *Biochim. Biophys. Acta 383,* 446-451.

Wong, K. L., and Kearns, D. R. (1974a), *Biopolymers 13,* 371-380.

Wong, K. L., and Kearns, D. R. (1974b), *Nature (London) 252,* 738-739.

Physical Characterization of a Ribosomal Nucleoprotein Complex†

Thomas R. Tritton*,‡ and Donald M. Crothers

ABSTRACT: The complex between ribosomal protein L24 and its RNA binding site (that region of the 23S RNA which the protein protects from ribonuclease digestion) has been studied by various physicochemical methods. The RNA is composed of two fragments of about 160 and 140 nucleotides which interact with each other to form the L24 binding site. Circular dichroism spectroscopy suggests that the two interacting fragments have a unique region of secondary structure which is not present in either of the two components alone; hence there are important structural interactions between regions of the RNA which are separated in the primary sequence. Addition of the L24 protein to the RNA site promotes a structural change associated with base unstacking, but with little or no change in the hydrogen-bonded base pairing. Heat activation is not required for complex formation. Thermal denaturation studies reveal a broad featureless transition and the amount of hypochromic change indicates that the RNA site contains less secondary structure than other RNAs such as tRNA and total rRNA. Temperature-jump relaxation measurements on the mechanism of unfolding of the RNA show a concerted melting of the entire secondary and tertiary structure, which is altered upon addition of the protein. A structural basis for this RNA-protein complex is discussed.

The *Escherichia coli* ribosome is made up of 55 different protein and 3 different RNA species. Highly specific interactions between these macromolecules are required for assembly and subsequently for function of the ribosome in protein synthesis. In general three types of interactions are possible: protein-protein, RNA-RNA, and protein-RNA. The topography of protein-protein interactions has been probed by a number of techniques, the most revealing of which have been the use of chemical cross-linking agents, affinity analogues, and specific antibodies. A recent review (Traut et al., 1974) demonstrates that a self-consistent picture of protein-protein interactions is rapidly emerging. Knowledge of the specific interactions among the RNA species and the arrangement of the RNA in the ribosomal architecture is very limited, although the nucleotide sequences of the three RNAs are either known (5S RNA; Brownlee et al., 1968) or in an advanced stage of analysis (16S and 23S RNA; Fellner, 1974). Our understanding of the nature of the RNA-protein interactions is at a more intermediate stage of development. About 20 of the 55 proteins bind specifically and individually (i.e., in the absence of one or more other ribosomal proteins) to one of the rRNAs. The stoichiometry of interaction and the approximate location of the specific binding region in the intact RNA sequence have been established for these proteins (reviewed by Zimmermann, 1974). In addition the solution conditions

† From the Department of Chemistry, Yale University, New Haven, Connecticut 06520. *Received March 29, 1976.*

‡ Present address: Department of Pharmacology, Yale University School of Medicine, New Haven, Connecticut 06510.